Plant aquaporin reconstituted proteoliposomes as nanosystem for resveratrol encapsulation

Lucia Yepes-Molina[1], Jose Teruel[2], Urban Johanson[3], and Micaela Carvajal[1]

[1]CEBAS
[2]University of Murcia
[3]Lund University

August 14, 2023

Abstract

Aquaporins (AQPs) are intrinsic membrane proteins responsible for facilitating water transport across biological membranes. AQPs found in plant membrane vesicles (MV) have been related to the functionality and stability of the vesicles. In this study, we focused on AQPs obtained from Brassica oleracea var. L. italica (broccoli) by the great potential for different biotechnological applications. To gain further insight into the role of AQPs in MV and advance the biotechnological applications of AQPs, we describe the heterologous overexpression of two broccoli AQPs (BoPIP1;2 and BoPIP2;2) in Pichia pastoris, resulting in the purification of both AQPs with high yield (0.14 and 0.99 mg per gram cells for BoPIP1;2 and BoPIP2;2, respectively). We reconstituted purified AQPs in liposomes to study their functionality, showing no changes in size compared to liposomes. BoPIP2;2 facilitated water transport, which was preserved for seven days at 4oC and 25ºC but not at 37oC, whereas BoPIP1;2 did not enhance water transport across the proteoliposome membrane. Additionally, BoPIP2;2 was incorporated into liposomes to encapsulate a resveratrol extract in proteoliposome vesicles, resulting in increased entrapment efficiency compared to conventional liposomes. Molecular docking identified potential binding sites for resveratrol in PIP2s, highlighting the role of AQPs in the improved entrapment efficiency of resveratrol. Moreover, a modelling study was conducted, demonstrating interactions between a plant AQP and human integrin, which may be a benefit to increase contact and internalization by the human target cells. Thus, our results suggest that AQPs-based alternative encapsulation systems can be used in specifically target biotechnological applications.

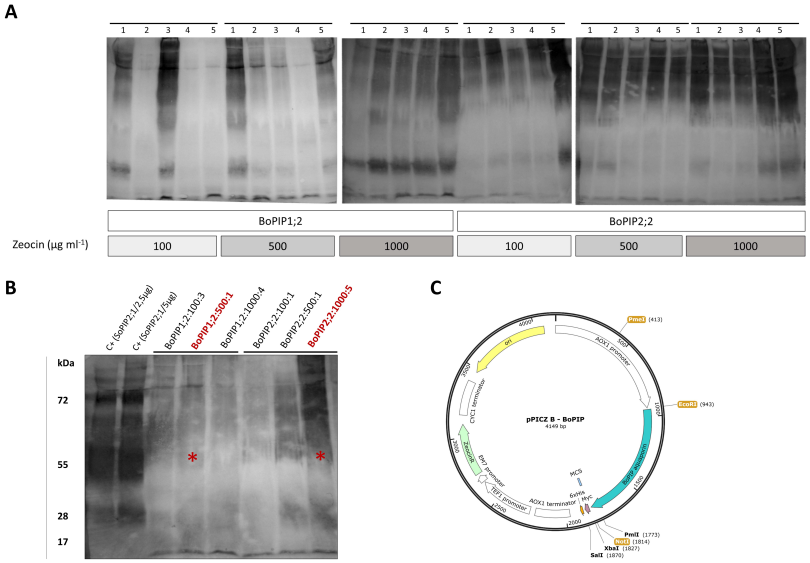

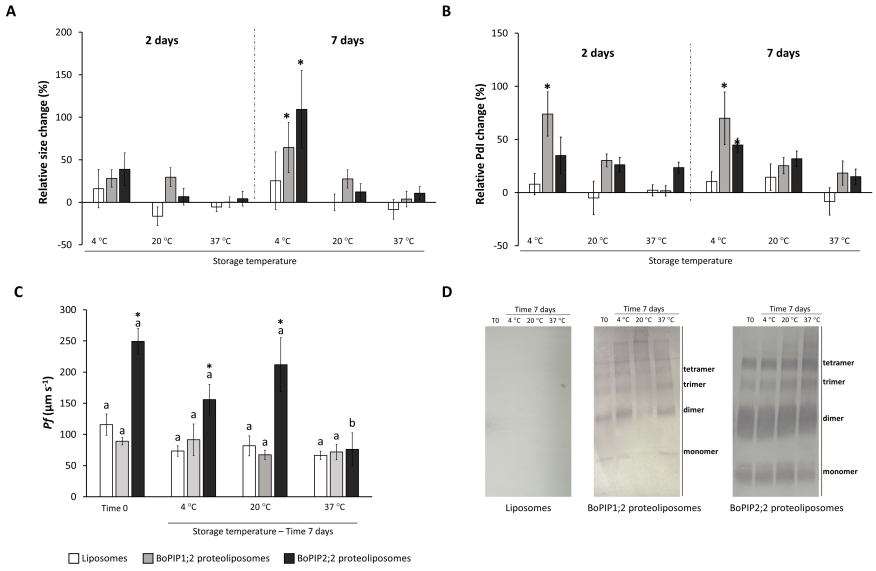

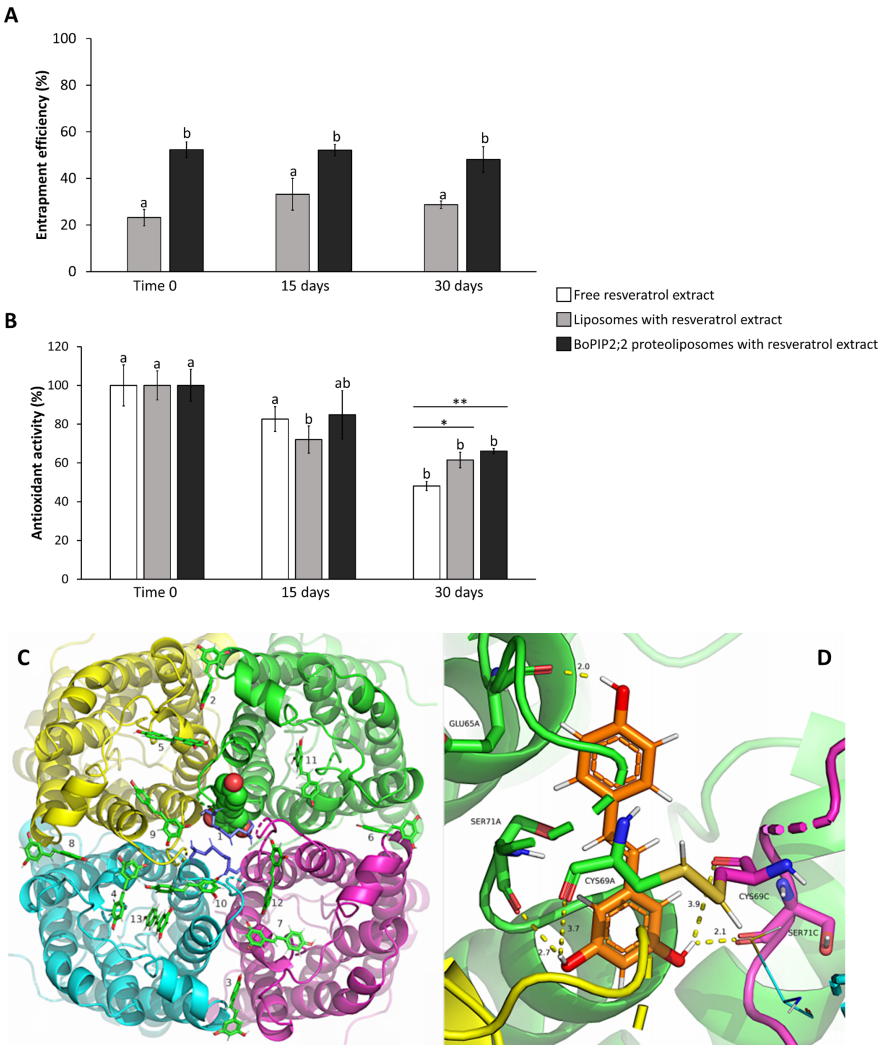

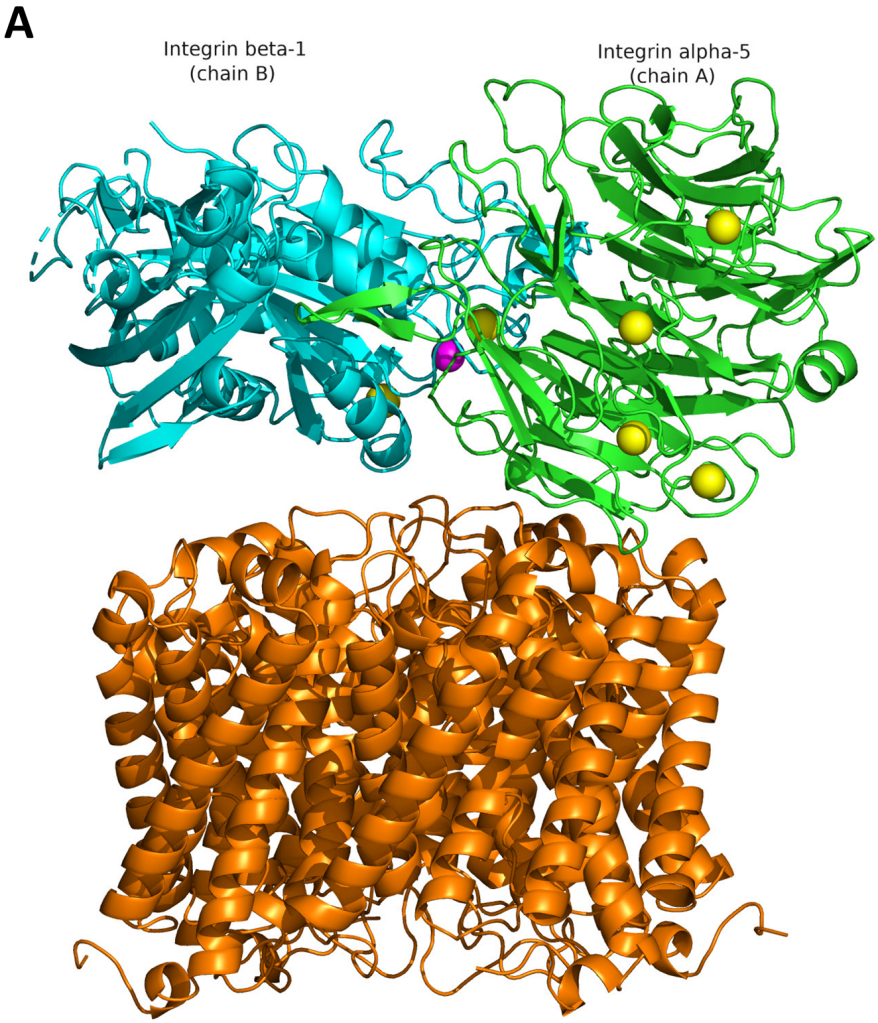

Plant aquaporin reconstituted proteoliposomes as nanosystem for resveratrol encapsulation

Lucia Yepes-Molina[1], Jose Antonio Teruel[2], Urban Johanson[3] & Micaela Carvajal[1*]

[1] Aquaporins Group. Centro de Edafologia y Biologia Aplicada del Segura (CEBAS), CSIC. Campus de Espinardo, E-30100 Murcia, Spain.

[2] Department of Biochemistry and Molecular Biology. Facultad de Veterinaria, Universidad de Murcia, E-30100 Murcia, Spain.

[3] Division of Biochemistry and Structural Biology, Center for Molecular Protein Science, Department of Chemistry, Lund University, Box 124, SE-221 00, Lund, Sweden.

*Corresponding author: mcarvaja@cebas.csic.es

Keywords: aquaporin, broccoli, membrane transporter reconstitution, proteoliposomes, nanocarrier.

ABSTRACT

Aquaporins, membrane proteins responsible for facilitating water transport, found in plant membrane vesicles (MV) have been related to the functionality and stability of MV. We focused on AQPs obtained from broccoli as they show potential for biotechnological applications. To gain further insight into the role of AQPs in MV, we describe the heterologous overexpression of two broccoli aquaporins (BoPIP1;2 and BoPIP2;2) in *Pichia pastoris*, resulting in their purification with high yield (0.14 and 0.99 mg per gram cells for BoPIP1;2 and BoPIP2;2). We reconstituted aquaporins in liposomes to study their functionality, and the size of proteoliposomes did not change concerning liposomes. BoPIP2;2 facilitated water transport, which was preserved for seven days at 4°C and at room temperature but not at 37°C. BoPIP2;2 was incorporated into liposomes to encapsulate a resveratrol extract, resulting in increased entrapment efficiency compared to conventional liposomes. Molecular docking was utilized to identify binding sites in PIP2s for resveratrol, highlighting the role of aquaporins in the improved entrapment efficiency. Moreover, interactions between plant AQP and human integrin was shown, which may be a benefit to increase internalization by the human target cells. Our results suggest aquaporins-based alternative encapsulation systems can be used in specifically target biotechnological applications.

1. INTRODUCTION

Aquaporins (AQPs), transmembrane proteins with an essential role in biological functions [1], primarily regulate water transport and maintain homeostasis though membrane water permeability adjustment [2,3]. These proteins are found in membrane vesicles (MV) isolated from natural sources, including *Brassica oleracea* var. L. *italica* (broccoli), studied by our group [4–6]. These MV have potential applications in cosmetics and pharmacology, as they interact with human cell membranes and enhancing bioactive compound uptake [7, 8]. AQPs contribute to MV stability and interact with bioactive compounds like glucoraphanin and sulforaphane, improving encapsulation [4,6,9,10]. Despite promising applications, aspects like AQPs' role in vesicle stability require further exploration.

Initially used as in vitro membrane models, liposomes have gained traction due to their biocompatibility, biodegradability [11], and ability to encapsulate hydrophilic and lipophilic compounds [12]. This versatility has extended their use to carrying unstable compounds like natural bioactive extracts. Whereas liposomes as nanocarriers are well-studied, proteoliposomes (liposomes with proteins) remain relatively unexplored, presenting a wide-open field for research. Proteins could give more stability to the nanosystem and, specifically AQPs, could improve the encapsulation because of their interaction with bioactive compounds

[5,10]. Hence, AQPs-containing proteoliposomes stand as a promising avenue to delve into MV stability and offer a viable nanocarrier solution.

The most efficient method to obtain pure membrane proteins is the heterologous expression in the methylotrophic yeast *Pichia pastoris* (renamed *Komagataella phaffii*) [13–16]. Although this system provides high yields, different factors may influence recombinant expression levels and subsequent protein purification; therefore, it is necessary a custom process for each protein of interest. Factors conditioning the level of gene expression are the properties of the nucleotide sequence, the mode of insertion of the sequence into the genome, or the culture conditions. To obtain the highest protein yields, the insertion of multiple copies of recombinant genes must be achieved [17,18], and for this, a strategy is to screen or select for different levels of antibiotic resistance, as this will correlated with the number of plasmids introduced into the genome. Regarding the purification of proteins, in the case of AQPs it is necessary to keep the protein in solution. For this, detergents are mandatory, and the selection of detergent is a critical step since the detergent properties will affect, on the one hand, the detergent removal efficiency and, on the other hand, the stability of proteins. Purified AQPs reconstituted into liposomes is one of the most used strategies to study different functionalities of these channel proteins, [19,20], but these studies could also bring different biotechnological results. For example, AQPs reconstituted in liposomes were employed to design water purification filters [21].

In the fields of cosmetics and pharmaceuticals, using natural sources to obtain bioactive compounds has gained significant interest. Phenolic extracts like resveratrol-enriched extract are notable for their antioxidant and anti-inflammatory properties [22]. However, their limited water solubility and bioavailability can hinder their effectiveness [23]. Encapsulating these extracts in liposomes provides a solution to overcome these challenges [24]. Efficient release of these encapsulated contents into target cells is crucial, highlighting the role of liposome-cell interaction. Membrane proteins, like integrins, are key for internalization [25], are responsible for internalization of exovesicles, and there is evidence suggesting that human AQP2 is involved in cell-cell adhesion through its interactions with integrins [26]. Thus, exploring the interaction between AQPs and integrins is an intriguing research direction, as incorporating AQPs into liposomes may facilitate the binding of proteoliposomes to cells.

Considering this background, the primary objective of this study is to investigate the functionality and properties of two AQPs from *Brassica oleracea* (BoPIP1;2 and BoPIP2;2). Firstly, we describe the successful overexpression of these proteins in *P. pastoris* and their purification. Subsequently, we evaluate the functionality of the reconstituted AQPs in liposomes and conduct a size stability assay. In addition, we explore the potential application of BoPIP2;2

proteoliposomes as carriers for a resveratrol extract. To determine the role of AQPs in the encapsulation capacity of proteoliposomes and their interaction with target human cells, we perform molecular docking assays.

2. EXPERIMENTAL SECTION

Recombinant protein overproduction in *Pichia pastoris*

Plasmid construction and cloning

Pichia pastoris vector pPICZB with BoPIP1;2 (GenBank accession XM_013780569.1) and BoPIP2;2 (XM_013767039.1) were purchase from Bionova cientifica S.L. (Madrid, Spain). Sequences were modified to optimize the start codon*,* ATG was replaced by aaaATGtct, and the original stop codon was omitted to allow a C-terminal translational fusion with the vector encoded Myc epitope and 6×His tag. Flanking restriction sites were added for subsequent cloning in pPICZB (5' EcoRI – GAATTC and 3'NotI – GCGGCCGC). The resulting plasmids were linearized by PmeI (GTTTAAAC) and were transformed into competent wild-type *P. pastoris* strain X-33 by electroporation according to EasySelect™ Pichia Expression Kit Manual (Invitrogen). Transformants were selected on YPDS (1% w/v yeast extract, 2% w/v peptone, 2% w/v dextrose, 1 M sorbitol) agar plates containing 100 μg mL^{-1} zeocin. After 5 days, colonies from the same transformation event were pooled and resuspended in YPDS medium and plated onto YPD agar plates containing 100, 500, and 1000 μg mL^{-1} zeocin to select for clones with higher resistance levels. 8 colonies from each construct and zeocin concentration were streaked for single-cell colonies to stabilize the transformation and 5 representative clones were analysed and assigned IDs describing the isoform, the antibiotic level, and the clone number (e. g. BoPIP1;2:100:1).

Small and large scale expression

A small-scale expression screen was performed to analyze the expression levels in *P. pastoris* clones selected at different antibiotic concentrations [18]. Transformants were grown in BMGY medium [1% (w/v) yeast extract, 2% (w/v) peptone, 100 mM potassium phosphate pH 6.0, 1.34% (w/v) yeast nitrogen base, 4×10^{-5}% (w/v) biotin, 1% (v/v) glycerol] at 28°C overnight. Cells were harvested and resuspended in BMMY medium [1% (w/v) yeast extract, 2% (w/v) peptone, 100 mM potassium phosphate pH 6.0, 1.34% (w/v) yeast nitrogen base, 4×10^{-5}% (w/v) biotin, 0.5% v/v methanol] to an optical density at 600 nm (OD_{600}) of 1. Cells were incubated and induction with methanol was maintained for 3 days (addition of fresh methanol every day). Cells corresponding to 20 OD_{600} units were harvested (16,000 x g, 5 min) and stored at -80°C. The pellets were resuspended in cold breaking buffer [50 mM $NaPO_4$ pH 7.4, 1 mM EDTA, 5% (v/v) glycerol, 1 mM PMSF], and broken by adding glass beads and vortexing 8 x 30 s with cooling

sessions. The lysate was centrifuged (18,000 x g, 5 min, 4°C) and the supernatants with the crude cell extracts were analysed for BoPIP1;2 or BoPIP2:2 content by Western-Blot. Cell extracts were mixed with 3.33 x SDS loading buffer [250 mM Tris-HCl pH 6.8, 40% (v/v) glycerol, 8% (w/v) SDS, 2.37 M β-mercaptoethanol, 0.1% (w/v) Bromophenol Blue]. A clone expressing SoPIP2;1 was used as a reference [27]. Protein was separated on 4-12% gradient SDS gels (Mini-PROTEAN® TGX™, Bio-Rad) and transferred to polyvinylidene difluoride (PVDF) membranes (Bio-Rad). Recombinant proteins were visualized by immunodetection (Primary Ab; mouse anti-6xHis-tag, Clonotech, and secondary Ab; polyclonal goat anti-mouse IgG alkaline phosphatase, Sigma). One transformant for each construction was chosen for large-scale culture.

The selected transformants were cultured on large-scale using a 3 L benchtop fermenter (Belach Bioteknik). BoPIP1;2 and BoPIP2;2 *P. pastoris* pre-cultures in BMGY were incubated at 30°C and 150 rpm overnight. 150 mL culture was added to 1.5 L basal salt medium [28] supplemented with 6.5 ml PTM_1 salts [29]. When glycerol was consumed a feed with 50% (v/v) glycerol with 1.2% (w/v) PTM_1 salts was initiated. After 6 h, the expression of AQPs was induced with 100% methanol with 1.2% (w/v) PTM_1 salts. After 50 h the culture reached an OD_{600} of 400 and cells were harvested by centrifugation (10,000 x g, 24 min, 4°C). Samples were collected at different times from the fermenter, normalized to contain the same OD_{600} units, and analysed by Western-Blot.

AQPs purification from *Pichia pastoris*

Membrane Pichia pastoris preparation

Cells were resuspended in cold breaking buffer, and breaking in a BeadBeater (BioSpec Products) with glass beads by 12 x 30 s runs with cooling sessions. Cell debris were removed by centrifugation (10,000 x g, 30 min, 4°C). The crude membrane fraction was collected by ultracentrifugation (186,400 x g, 1 h, 4°C), and resulting pellets were resuspended in cold buffer A [20 mM HEPES-NaOH pH 7.8, 50 mM NaCl, 10% (v/v) glycerol, 2 mM β-mercaptoethanol]. A urea membrane wash procedure, as described by Fotiadis et al. (2001) [30], was carried out. Protein concentration was assayed according to Bearden [31].

Detergent screening

Membranes were diluted with buffer A to 4 mg mL^{-1} and mixed with different detergents in a dropwise manner to a final protein concentration of 2 mg mL^{-1} and a final detergent concentration of 10 x critical micelle concentration (CMC) [5.3 % n-Octyl-β-D-glucoside (OG), 2% n-nonyl-β-D-glucoside (NG), 0.47 % n-dodecylphosphocholine (Fos-choline-12) and 0.087% n-dodecyl-β-D-maltopyranoside (DDM), (from Anatrace)]. The non-solubilized and solubilized proteins were separated by ultracentrifugation (150,000 x g, 30 min, 4°C), and checked through Coomassie and Western-Blot.

Protein solubilization and Ni-NTA affinity chromatography

The solubilized proteins were mixed with 10 mM imidazole and 4 mL of Ni-NTA agarose (Qiagen) preequilibrated with buffer A + 3 x CMC OG, and incubated overnight at 4°C. Ni-NTA agarose with proteins was packed into empty PolyPrep-columns (Bio-Rad) and washed with 10-bed volumes of buffer B [20 mM HEPES-NaOH pH 7.8, 300 mM NaCl, 10% (v/v) glycerol, 5 mM β-mercaptoethanol] with 3 x CMC OG and 30 mM imidazole. The proteins were eluted in buffer B supplemented with 3 x CMC OG and 300 mM imidazole in the first elution, and with 500 mM imidazole in the second elution. Fractions were analysed by Coomassie staining and Western-Blot. The protein concentration was determined by A_{280} in Nanodrop, applying the extinction coefficient of 46.41 M^{-1} cm^{-1} for BoPIP1;2 and 46.87 M^{-1} cm^{-1} for BoPIP2;2, and considering their molecular weights of 33.73 kDa and 33.14 kDa, respectively (Expasy ProtParam [32]).

AQPs reconstitution into proteoliposomes

Purified AQPs were reconstituted into proteoliposomes by mixing them with *Escherichia coli* lipids (Avanti Polar Lipids, Alabaster, AL., USA) solubilized in 5% OG. The lipid-to-protein ratio (LPR) was set at 30, and the reconstitution was performed in Stopped-Flow Buffer [20 mM Tris-HCl, pH 8.0, 100 mM NaCl, 2 mM dithiothreitol (DTT), 0.03% NaN_3] with a final lipid concentration of 2 mg mL^{-1}. The mixture was incubated for 10 min at RT with gentle mixing. OG was removed with Bio-Beads (2 h of incubation). The reconstituted proteoliposomes were extruded 11 times through an extruder (Avanti Polar Lipids) using a 200-nm Whatman polycarbonate membrane. Control liposomes were made in the same manner without protein. The size and polydispersity index (PDI) were measured using dynamic light scattering (DLS) on a Malvern Zetasizer NanoZS instrument at 25°C (3 measurements of 13 runs each were taken). Immunoblotting against 6xHis-tag was done to confirm the integrity of the proteins. To assess the functional characterization of both AQPs, the osmotic water permeability (*Pf*) was measured in a PiStar-180 Spectrometer (Applied Photophysics, Leatherhead, UK), as previously described by Barrajón-Catalán et al. (2010) [33]. All these measurements were performed at different time points (0 h, 48 h, and 1 week) and at different storage temperatures (4°C, RT, and 37°C).

Resveratrol extract encapsulation in liposomes and BoPIP2;2 proteoliposomes

E. coli lipids were dried with nitrogen gas, and the resulting thin lipid film was reconstituted with PBS to a final concentration of 2 mg ml^{-1}. The reconstitution process involved the addition of 1 mg ml^{-1} of resveratrol extract and purified BoPIP2;2 (LPR = 30). For the control group, the same amount of Buffer A was added to form liposomes with the extract. The solutions were sonicated for 10 min. To determine the entrapment efficiency (EE) of resveratrol extract, 1 ml of each sample was pelleted by centrifugation (10,000 x g, 30 min), and the pellet was

resuspended in PBS. The content of the resveratrol extract in the pellet and supernatant was measured by checking the absorbance at 280 nm. DLS was used to determine the size and PDI. The antioxidant activity was determined using the DPPH assay [34]. All these parameters were measured in samples at the initial time and after storage for 15 and 30 days at 4°C.

Molecular docking of resveratrol and integrin with aquaporin

Molecular docking of resveratrol (PubChem Substance and Compound database [35], CID 445154) was performed on the outer surface of AQP tetramer, which 3D structure was taken from the Protein Databank (PDB ID: 4JC6) [36], which correspond to the aquaporin SoPIP2 from spinach (2.15 Å). The protein structure was prepared by adding all hydrogen atoms, removing octyl β-D-glucopyranoside, mercury and cadmium ions as well as water molecules, and selecting one of the two tetramers (chains A-D). Gasteiger atom charges (pH 7) were assigned to both resveratrol and aquaporin, and rotatable bonds in resveratrol, were assigned using AutoDockTools4 software [37,38]. Docking was performed using the AutoDock 4.2.6 suite [38]. Lamarkian Genetic Algorithm was chosen to search for the best conformers. The number of independent docking was set to 1000, the maximum number of energy evaluations to 2,500,000, and the population size to 150. Grid parameter files were built using AutoGrid 4.2.6 [39]. The grid box was selected to restrict docking to the outer surface of the AQP tetramer. PyMOL 2.3.0 [40] was employed to edit and inspect the docked conformations and Wrap-Shake [41] to inspect multiple binding conformations.

Molecular docking of integrin (PDB ID: 4WJK), corresponding to the crystal structure of a four-domain α5β1 headpiece fragment, was also carried out on the outer surface of aquaporin as a tetramer. Protein structure was adapted for docking. Molecular docking was done with HADDOCK server [42,43]. Docking conformation was selected by the HADDOCK scoring function and ignoring those integrin conformations not located in the outer surface of aquaporin. Prediction of binding affinity of the selected conformation was calculated by using PRODIGY [44].

3. RESULTS

BoPIP1;2 and BoPIP2;2 production in *Pichia pastoris*: cell yield and membrane recovery

To obtain purified BoPIP1;2 and BoPIP2;2, the proteins were transformed into the methylotrophic yeast *P. pastoris* using the construction outlined in Figure 1C. To optimize the production of purified proteins at a small scale before proceeding to large-scale production, various parameters were examined. To screen for high-yielding clones, five clones for each construct and each of the three different zeocin selection concentrations were analyzed by

immunoblotting (Figure 1A). The best clones were selected and compared for expression levels in the same western-blot (Figure 1B). Based on the expression levels of each isoform, the clone with the highest expression was chosen for further experiments. In the case of BoPIP1;2, the best results were obtained with a clone selected at 500 µg zeocin mL^{-1}. For BoPIP2;2, the expression level showed a positive correlation with the zeocin concentration, and the highest expression was achieved a with a clone selected on zeocin at 1000 µg mL^{-1}.

The selected clones for each AQP were produced on a large scale. The cell biomass was monitored at different time points, and after 72 h, a similar amount of biomass was reached for both isoforms (Figure 1D-F). At the end of fermentation, cell and protein yield were calculated for each AQP isoform overexpressed in *P. pastoris*. 1.5 L of culture gave 590 and 655 g of cells harvested 72 h after induction for BoPIP1;2 and BoPIP2;2, respectively. Regarding protein yield, after breaking cells, from 1.5 L of culture 4100 and 6300 mg of total membrane proteins were obtained, corresponding to 7 and 10 mg per gram cells for BoPIP1;2 and BoPIP2;2, respectively.

Membrane proteins solubilisation and aquaporins purification

A solubilization screen was conducted to determine the most effective detergent for large-scale solubilization. Among the tested detergents, OG demonstrated the best solubilization efficiency for both proteins. Although FC-12 showed better solubilization, it was not selected for large-scale use due to its potential interference with the affinity chromatography step during protein purification (Figure S1). The solubilized proteins were then purified using affinity chromatography through the added His-tag at the C-terminus of the recombinant BoPIP1;2 and BoPIP2;2. The purification process was checked by Coomassie-stained and Western-blot (Figure 1G-H), which demonstrated the enrichment of BoPIP1;2 and BoPIP2;2 in the elution fractions. Approximately 0.14 mg and 0.99 mg of pure proteins per gram of cells were obtained for BoPIP1;2 and BoPIP2;2, respectively. Both purified AQPs exhibited a similar pattern: monomers, dimers, trimers, and tetramers.

Reconstitution of BoPIP1;2 and BoPIP2;2 in liposomes

BoPIP1;2 and BoPIP2;2 were reconstituted in liposomes, and the resulting proteoliposomes and empty liposomes were characterized (Table 1). Sizes between 255 and 296 nm and PDI of 0.32-0.34 were obtained without significant differences between samples. To assess the functionality of the purified and reconstituted proteins, water channel activity was determined using stopped-flow spectrophotometry. BoPIP2;2 proteoliposomes showed an increase in both rate constants and *Pf* compared to empty liposomes, indicating that BoPIP2;2 is functional and capable of channelling water. No significant differences were found between BoPIP1;2 proteoliposomes and empty liposomes. Furthermore, a stability assay was conducted to assess

the behaviour of liposomes and proteoliposomes reconstituted with AQPs over time at different temperatures. Empty liposomes and proteoliposomes did not change their size after two days of storage at any temperature. However, significant size changes were observed in both types of proteoliposomes after seven days of storage at 4 °C. In contrast, both empty liposomes and proteoliposomes maintained their size when stored at higher temperatures (Figure 2A). An increase in PDI was observed after seven days of storage at 4 °C specifically for proteoliposomes, but not for empty liposomes. Besides, this increase in PDI was also observed in BoPIP1;2 proteoliposomes already after two days at 4 °C (Figure 2B).

The functionality of AQPs was also assessed after seven days of storage at the same three temperatures (Figure 2C). Initially, both liposomes and BoPIP1;2 proteoliposomes had the same *Pf*, around 100 µm s^{-1}, and both samples maintained these values of *Pf* in all tested conditions after seven days. BoPIP2;2 proteoliposomes had a higher *Pf* (250 µm s^{-1}), which remained unchanged after seven days at 4 °C and 20 °C, but a significant decrease was observed at 37 °C. Furthermore, the protein levels and the arrangement pattern of AQPs (monomers, dimers, trimers, and tetramers) were analysed by western-blot under the same storage conditions (Figure 2D). No significant changes in protein abundance of BoPIP1;2 were observed at 4 °C and 37 °C and at any condition in case of BoPIP2;2. Regarding AQP arrangement, no significant differences were observed after seven days of storage.

Encapsulation of resveratrol extract in BoPIP2;2 proteoliposomes

Resveratrol extract was encapsulated in empty liposomes and BoPIP2;2 proteoliposomes to assess the effect of protein incorporation on EE. BoPIP2;2 was chosen for high production efficiency and functionality. Various parameters were measured for the encapsulated extract in both liposomes and BoPIP2;2 proteoliposomes (Table 2). BoPIP2;2 proteoliposomes exhibited a 2.25-fold increase in EE compared to liposomes. As for size and PDI, these values were higher for BoPIP2;2 proteoliposomes containing the encapsulated extract. The antioxidant activity did not show differences between free resveratrol extract and extract encapsulated in both empty liposomes and proteoliposomes. The EE remained stable for 30 days, regardless of whether the extract was encapsulated in liposomes or proteoliposomes (Figure 3A). In terms of antioxidant activity, there was a decrease observed after 30 days of storage; however, the activity was higher when the resveratrol extract was encapsulated in liposomes and when it was encapsulated in proteoliposomes (Figure 3B).

Molecular docking of resveratrol and integrin with PIP2 aquaporin

A molecular docking study was performed to investigate the potential role of AQPs in the increased percentage of resveratrol encapsulation in liposomes when AQPs are included in the

formulation. The aim was to elucidate if AQPs have binding sites for resveratrol, the target molecule in this study. The results of this *in silico* study revealed multiple binding conformations between the resveratrol and AQP (Figure 3C). Table 3 presents a summary of all poses and the AQP residues involved in the interaction. Among the different poses, one was found in the central pore formed by the four monomers of AQP in the membrane, and this pose exhibited the lowest binding energy (-5.58 kcal/mol). The entrance to this pore is blocked by two disulphide bridges between Cys 69, however, resveratrol could be located next to a disulphide bridge in a gap formed in the structure (Figure 3D). The residues contributing to this conformation were identified in several monomers of the protein, namely GLU65A, CYS69A, SER71A, and SER71C, where A and C represent different protein monomers (Figure 3D).

On the other hand, an *in silico* modelling was performed between plant PIP2 aquaporin and human integrin, and a 3D representation is depicted in Figure 4. The best binding conformation exhibited a free energy of binding of -10.4 kcal/mol, corresponding to a Kd of 24 nM. The residues of both proteins involved in the binding are summarized in Table 4. The interaction primarily occurs between the alpha-5 integrin (A-chain) and two aquaporin monomers (A and C).

4. DISCUSSION

AQPs are pivotal in facilitating water transport through biological membranes, holding significance for diverse biological processes [3]. Despite significant progress in understanding AQPs, many aspects of their regulation and functions remain unclear. In-depth investigations using *in vitro* assays with pure proteins have provided valuable insights into their mechanisms and properties [45]. The production of large quantities of pure proteins is of great interest, particularly from a physiological perspective. Pure proteins are essential for crystallography studies to determine the three-dimensional structure of proteins, shedding light on their functional mechanisms. Additionally, they are crucial for studying the functionality of transmembrane transporters or channels, such as AQPs, through reconstitution in artificial liposomes. Moreover, the production of pure proteins holds significant promise in the biotechnology industry [46]. One notable application is in the development of devices and technologies aimed at enhancing water filtration and purification processes [21] or for the development of products with moisturising and stabilising properties. Heterologous expression has proven the most efficient method for attaining pure proteins. Obtaining proteins from natural sources often results in poor yields due to low expression levels and protein loss during purification. Challenges intensify when purifying specific AQP isoforms due to their numerous isoforms. For instance, in broccoli, more than 60 AQP genes have been described with specific

but overlapping expression patterns [47]. Methylotrophic yeast *P. pastoris* has emerged as a superior host for recombinant protein expression compared to E. coli, particularly for membrane proteins [14]. As a eukaryote, P. pastoris ensures proper folding and post-translational modifications of proteins [48].

In our investigation, we optimized the production protocol for BoPIP1;2 and BoPIP2;2 proteins from *B. oleracea* using *P. pastoris* as the expression system. We focused on enhancing translation initiation by replacing the start codon ATG [49] with the sequence aaaATGtct, known for its suitability in yeast expression systems [50]. Furthermore, we screened clones at different zeocin concentrations to identify those with the highest gene dosage, as gene dosage correlates with protein production [18]. Zeocin concentration of 500 µg mL^{-1} displayed the best protein expression for BoPIP1;2, as shown Nordén et al. (2011) for SoPIP1;2. In case of BoPIP2;2, we selected clones with higher expression levels at 1000 µg zeocin mL^{-1}, similar to previous studies with other human and plant AQPs [18]. These results underscore the importance of protocol optimization in attaining high protein yields and provide valuable insights for future studies on AQP expression in heterologous systems. Controlled growth is crucial for protocol optimization, with monitored conditions in fermenters being ideal for large-scale production. An effective purification approach is also vital to sustain high yields, and detergent screening is imperative to obtain functional proteins. In this study, OG was chosen as the best option after FC-12, which is considered a harsher detergent, with a higher risk of compromising the fold of the protein of interest. OG is commonly used for solubilizing AQPs due to their stability in glucopyranosides [51], as observed with PIP2;4 from *A. thaliana* [20] or PIP2;1 from *S. oleracea* [52]. Yields obtained in our study could be consider exceptional compared to previous bibliography on the purification of AQPs [53]. From yeast overexpressed BoPIP1;2, 0.14 mg g^{-1} of pure protein were obtained, and for BoPIP2;2, the yield was even higher, 0.99 mg per gram of yeast cell. These yields are consistent with the production range of 0.1-0.5 mg of pure protein per gram of yeast cell reported by Al-Jubair et al. (2022) [54].

At this stage, AQPs were reconstituted into liposomes, which have been extensively investigated from various perspectives. They serve as experimental models for investigating cell membrane science, membrane proteins, and as carriers for bioactive compounds. Regarding functionality, BoPIP1;2 exhibited similar water transport to control liposomes, while BoPIP2;2 displayed a two-fold higher *Pf*. Similar behaviour has been observed in previous studies with PIP2 proteins, such as AtPIP2;4 or SoPIP2;1 reconstituted in liposomes [20] or VvTnPIP2;1 and VvTnPIP2;3 expressed in yeasts [55]. Conversely, PIP1 have been known to exhibit limited water transport capabilities for many years [56]. These varying results indicate that multiple factors

influence the functionality of PIP1, including lipid composition of membranes, pH, and heterotetramerization with other AQPs [45].

Considering the potential biotechnological applications of AQPs [57,58], investigating protein aggregation becomes a common challenge. In the stability assay conducted over one week at different temperatures, it was observed that the size and PDI of the proteoliposomes, compared to the control liposomes, remained unaffected except when stored at 4°C. Although protein aggregation typically correlates with higher temperatures, it can occur at near 0°C, with both types following similar unfolding mechanisms [59]. Besides protein aggregation, fusion between proteoliposomes mediated by AQPs' interaction, forming larger vesicles, should be acknowledged. Moreover, proteoliposome functionality, is crucial to consider in stability assessment. The *Pf* of BoPIP2;2 proteoliposomes remained unchanged when stored at 4°C and RT, but a decrease in *Pf* was observed after storage at 37°C, reaching a level comparable to that of the control liposomes. Thus, changes in size as well as homogeneity and retained function must be considered when finding optimal storage conditions.

The utilization of AQPs proteoliposomes offer a promising strategy for enhancing the stability and bioactivity of unstable bioactive extracts, like resveratrol-enriched grape extract, with potential applications in pharmacy and cosmetics [60]. Achieving higher EE is crucial for improved cargo absorption and bioavailability [61]. Our study revealed a 2.25-fold higher EE of resveratrol extract in BoPIP2;2-containing proteoliposomes compared to empty liposomes, remaining stable after 30 days, and considering that without extract there is no significant difference in the size of liposomes and BoPIP2;2 proteoliposomes. This might result from direct interactions between resveratrol molecules and AQPs. This hypothesis is supported by results obtained from molecular docking assays, which indicate potential binding sites between PIP2 protein and the resveratrol molecule, with the most probable interaction occurring at the central pore of the AQP tetramer. Similar interaction between proteins and resveratrol have been reported in other studies [62]. Moreover, AQPs have been demonstrated to interact with different molecules and stabilize them *in vitro*, such as the glucosinolate glucoraphanin [5]. Molecular docking studies have also shown electrostatic, hydrogen bonding, and non-polar interactions between PIP2 aquaporin and glucoraphanin [5], as well as with sulforaphane [10]. Thus, BoPIP2;2 likely plays a significant role in the entrapment of resveratrol, although in addition to the interaction with AQP, the fact that aquaporin makes somewhat larger vesicles may also contribute to the higher encapsulation efficiency. Therefore, further studies are needed to investigate this aspect in more detail. It is worth noting that the docking was performed only on the extracellular surface of AQP, and an equal distribution of proteins

between the inner and outer surfaces of the proteoliposomes is expected. This could be relevant in understanding the actual effect occurring under *in vitro* and *in vivo* conditions.

Determining the interactions of these liposomes with the target cells is crucial considering cosmetics of pharmacological application. Our results with docking revealed the interaction between the AQPs present in our liposomes and the integrins found on human cell membranes. The possibility of this binding offers advantages, as integrins are molecules directly involved in the internalisation of exovesicles, thereby potentially enhancing the absorption of the encapsulated active compounds by the target cells [63]. This interaction holds significant promise for improving the efficacy of the encapsulation system in delivering bioactive compounds to the desired targets cells.

In summary, this study successfully optimized the overexpression and purification process of two AQPs from *Brassica oleracea* (BoPIP1;2 and BoPIP2;2). Among the proteins studied, PIP2 demonstrated not only higher production and purification yields but also exhibited higher water transport activity. It was observed that the presence of AQPs in the system significantly increased the EE of the extract. Furthermore, *in silico* experiments revealed promising AQP binding possibilities, particularly with integrins found on human cell membranes. This interaction is crucial for the internalization of proteoliposomes by target cells, suggesting potential advantages for enhancing the absorption of encapsulated active compounds. Overall, these findings advance AQP-based systems for encapsulating and delivering bioactive compounds. The study underscores AQPs' potential in biotechnological applications, particularly in interactions with target cells to enhance encapsulated compound stability and bioavailability.

5. REFERENCES

1. Finn, R. N., & Cerdá, J. (2015). Evolution and functional diversity of aquaporins. *Biological Bulletin*, *229*(1), 6–23. https://doi.org/10.1086/BBLv229n1p6

2. Gomes, D., Agasse, A., Thiébaud, P., Delrot, S., Gerós, H., & Chaumont, F. (2009). Aquaporins are multifunctional water and solute transporters highly divergent in living organisms. *Biochimica et Biophysica Acta - Biomembranes*, *1788*(6), 1213–1228. https://doi.org/10.1016/j.bbamem.2009.03.009

3. Maurel, C., Verdoucq, L., Luu, D.-T., & Santoni, V. (2008). Plant aquaporins: membrane channels with multiple integrated functions. *Annual Review of Plant Biology*, *59*, 595–624. https://doi.org/10.1146/annurev.arplant.59.032607.092734

4. Chalbi, N., Martínez-Ballesta, M. C., Youssef, N. Ben, & Carvajal, M. (2015). Intrinsic stability of Brassicaceae plasma membrane in relation to changes in proteins and lipids as a response to salinity. *Journal of Plant Physiology*, *175*(1), 148–156. https://doi.org/10.1016/j.jplph.2014.12.003

5. Martínez Ballesta, M. C., Pérez-Sánchez, H., Moreno, D. A., & Carvajal, M. (2016). Plant plasma membrane aquaporins in natural vesicles as potential stabilizers and carriers of glucosinolates. *Colloids and Surfaces B: Biointerfaces*, *143*, 318–326. https://doi.org/10.1016/j.colsurfb.2016.03.056

6. Martínez Ballesta, M. C., García-Gomez, P., Yepes-Molina, L., Guarnizo, A. L., Teruel, J. A., & Carvajal, M. (2018). Plasma membrane aquaporins mediates vesicle stability in broccoli. *PLOS ONE*, *13*(2), 1–19. https://doi.org/10.1371/journal.pone.0192422

7. Yepes-Molina, L., Martínez-Ballesta, M. C., & Carvajal, M. (2020). Plant plasma membrane vesicles interaction with keratinocytes reveals their potential as carriers. *Journal of Advanced Research*, *23*, 101–111. https://doi.org/10.1016/j.jare.2020.02.004

8. Yepes-Molina, L., & Carvajal, M. (2021). Nanoencapsulation of sulforaphane in broccoli membrane vesicles and their in vitro antiproliferative activity. *Pharmaceutical Biology*, *59*(1), 1490–1504. https://doi.org/10.1080/13880209.2021.1992450

9. Yepes-Molina, L., & Carvajal, M. (2021). Nanoencapsulation of sulforaphane in broccoli membrane vesicles and their in vitro antiproliferative activity. *Pharmaceutical Biology*, *59*(1), 1490–1504. https://doi.org/10.1080/13880209.2021.1992450

10. Yepes-Molina, L., Pérez-Jiménez, M. I., Martínez-Esparza, M., Teruel, J. A., Ruiz-Alcaraz, A. J., García-Peñarrubia, P., & Carvajal, M. (2022). Membrane Vesicles for Nanoencapsulated SulforaphaneIncreased Their Anti-Inflammatory Role on an In Vitro Human Macrophage Model. *International Journal of Molecular Sciences*, *23*(4). https://doi.org/10.3390/ijms23041940

11. van Rooijen, N., & van Nieuwmegen, R. (1980). Liposomes in immunology: Multilamellar phosphatidylcholine liposomes as a simple, biodegradable and harmless adjuvant without any immunogenic activity of its own. *Immunological Investigations*, *9*, 243–256. https://doi.org/10.3109/08820138009065997

12. Schwendener, R. A. (2014). Liposomes as vaccine delivery systems: A review of the recent advances. *Therapeutic Advances in Vaccines*, *2*, 159–182. https://doi.org/10.1177/2051013614541440

13. Long, S. B., Campbell, E. B., & MacKinnon, R. (2005). Crystal structure of a mammalian voltage-dependent Shaker family K + channel. *Science*, *309*(5736), 897–903. https://doi.org/10.1126/science.1116269

14. Karbalaei, M., Rezaee, S. A., & Farsiani, H. (2020). Pichia pastoris: A highly successful expression system for optimal synthesis of heterologous proteins. *Journal of Cellular Physiology*, *235*(9), 5867–5881. https://doi.org/10.1002/jcp.29583

15. Kurtzman, C. P. (2009). Biotechnological strains of Komagataella (Pichia) pastoris are Komagataella phaffii as determined from multigene sequence analysis. *Journal of Industrial Microbiology & Biotechnology*, *36*(11), 1435–1438. https://doi.org/10.1007/s10295-009-0638-4

16. Heistinger, L., Gasser, B., & Mattanovich, D. (2020). Microbe Profile: Komagataella phaffii: a methanol devouring biotech yeast formerly known as Pichia pastoris. *Microbiology*, *166*(7), 614–616. https://doi.org/10.1099/mic.0.000958

17. Romanos, M., Scorer, C., Sreekrishna, K., & Clare, J. (1998). The generation of multicopy recombinant strains. *Methods in Molecular Biology (Clifton, N.J.)*, *103*, 55–72. https://doi.org/10.1385/0-89603-421-6:55

18. Nordén, K., Agemark, M., Danielson, J. J. T., Alexandersson, E., Kjellbom, P., & Johanson, U. (2011). Increasing gene dosage greatly enhances recombinant expression of aquaporins in Pichia pastoris. *BMC Biotechnology*, *11*, 47. https://doi.org/10.1186/1472-6750-11-47

19. Kirscht, A., Survery, S., Kjellbom, P., & Johanson, U. (2016). Increased permeability of the aquaporin SoPIP2;1 by mercury and mutations in loop a. *Frontiers in Plant Science*, *7*, 1249. https://doi.org/10.3389/fpls.2016.01249

20. Wang, H., Schoebel, S., Schmitz, F., Dong, H., & Hedfalk, K. (2020). Characterization of aquaporin-driven hydrogen peroxide transport. *Biochimica et Biophysica Acta - Biomembranes*, *1862*(2), 183065. https://doi.org/10.1016/j.bbamem.2019.183065

21. Sun, G., Chung, T. S., Jeyaseelan, K., & Armugam, A. (2013). Stabilization and immobilization of aquaporin reconstituted lipid vesicles for water purification. *Colloids and Surfaces B: Biointerfaces*, *102*, 466–471. https://doi.org/10.1016/j.colsurfb.2012.08.009

22. de Lima Cherubim, D. J., Buzanello Martins, C. V., Oliveira Fariña, L., & da Silva de Lucca, R. A. (2020). Polyphenols as natural antioxidants in cosmetics applications. *Journal of Cosmetic Dermatology*, *19*, 33–37. https://doi.org/10.1111/jocd.13093

23. Gambini, J., Inglés, M., Olaso, G., Lopez-Grueso, R., Bonet-Costa, V., Gimeno-Mallench, L., Mas-Bargues, C., Abdelaziz, K. M., Gomez-Cabrera, M. C., Vina, J., & Borras, C. (2015). Properties of Resveratrol: In Vitro and In Vivo Studies about Metabolism, Bioavailability, and Biological Effects in Animal Models and Humans. *Oxidative Medicine and Cellular Longevity*, *2015*, 837042. https://doi.org/10.1155/2015/837042

24. Figueroa-Robles, A., Antunes-Ricardo, M., & Guajardo-Flores, D. (2021). Encapsulation of phenolic compounds with liposomal improvement in the cosmetic industry. *International Journal of Pharmaceutics*, *593*, 120125. https://doi.org/10.1016/j.ijpharm.2020.120125

25. Gonda, A., Kabagwira, J., Senthil, G. N., & Wall, N. R. (2019). Internalization of Exosomes through Receptor-Mediated Endocytosis. *Molecular Cancer Research*, *17*(2), 337–347. https://doi.org/10.1158/1541-7786.MCR-18-0891

26. Chen, Y., Rice, W., Gu, Z., Li, J., Huang, J., Brenner, M. B., Van Hoek, A., Xiong, J., Gundersen, G. G., Norman, J. C., Hsu, V. W., Fenton, R. A., Brown, D., & Lu, H. A. J. (2012). Aquaporin 2 Promotes Cell Migration and Epithelial Morphogenesis. *Journal of the American Society of Nephrology*, *23*(9), 1506–1517. https://doi.org/10.1681/ASN.2012010079

27. Karlsson, M., Fotiadis, D., Sjövall, S., Johansson, I., Hedfalk, K., Engel, A., & Kjellbom, P. (2003). Reconstitution of water channel function of an aquaporin overexpressed and purified from Pichia pastoris. *FEBS Letters*, *537*, 68–72. https://doi.org/10.1016/S0014-5793(03)00082-6

28. Stratton, J., Chiruvolu, V., & Meagher, M. (1998). High cell-density fermentation. In *Pichia protocols* (pp. 107–120). Springer.

29. Bushell, M. E., Rowe, M., Avignone-Rossa, C. A., & Wardell, J. N. (2003). Cyclic fed-batch culture for production of human serum albumin in Pichia pastoris. *Biotechnology and Bioengineering*, *82*, 678–683. https://doi.org/10.1002/bit.10616

30. Fotiadis, D., Jenö, P., Mini, T., Wirtz, S., Müller, S. A., Fraysse, L., Kjellbom, P., & Engel, A. (2001). Structural characterization of two aquaporins isolated from native spinach leaf plasma membranes. *Journal of Biological Chemistry*, *276*, 1707–1714. https://doi.org/10.1074/jbc.M009383200

31. Bearden, J. C. (1978). Quantitation of submicrogram quantities of protein by an improved protein-dye binding assay. *BBA - Protein Structure*, *533*, 525–529. https://doi.org/10.1016/0005-2795(78)90398-7

32. Gasteiger, E., Hoogland, C., Gattiker, A., Duvaud, S., Wilkins, M. R., Appel, R. D., & Bairoch, A. (2005). Protein Identification and Analysis Tools on the ExPASy Server. In *The Proteomics Protocols Handbook* (pp. 571–607). https://doi.org/10.1385/1-59259-890-0:571

33. Barrajón-Catalán, E., Menéndez-Gutiérrez, M. P., Falco, A., Carrato, A., Saceda, M., & Micol, V. (2010). Selective death of human breast cancer cells by lytic immunoliposomes: Correlation with their HER2 expression level. *Cancer Letters*, *290*, 192:203. https://doi.org/10.1016/j.canlet.2009.09.010

34. Blois, M. S. (1958). Antioxidant determinations by the use of a stable free radical. *Nature*, *181*, 1199–1200. https://doi.org/10.1038/1811199a0

35. Kim, S., Thiessen, P. A., Bolton, E. E., Chen, J., Fu, G., Gindulyte, A., Han, L., He, J., He, S., Shoemaker, B. A., Wang, J., Yu, B., Zhang, J., & Bryant, S. H. (2016). PubChem Substance and Compound databases. *Nucleic Acids Research*, *44*(D1), D1202–D1213. https://doi.org/10.1093/nar/gkv951

36. Frick, A., Järvå, M., Ekvall, M., Uzdavinys, P., Nyblom, M., & Törnroth-Horsefield, S. (2013). Mercury increases water permeability of a plant aquaporin through a non-cysteine-related mechanism. *Biochemical Journal*, *454*(3), 491–499. https://doi.org/10.1042/BJ20130377

37. Sanner M. (1999). Python: a programming language for software integration and development. *Mol Graph Mode*, *17*(1), 57–61.

38. Morris, G. M., Huey, R., Lindstrom, W., Sanner, M. F., Belew, R. K., Goodsell, D. S., & Olson, A. J. (2009). AutoDock4 and AutoDockTools4: Automated docking with selective receptor flexibility. *Journal of Computational Chemistry*, *30*(16), 2785–2791. https://doi.org/10.1002/jcc.21256

39. Huey, R., Morris, G. M., Olson, A. J., & Goodsell, D. S. (2007). A semiempirical free energy force field with charge-based desolvation. *Journal of Computational Chemistry*, *28*(6), 1145–1152. https://doi.org/10.1002/jcc.20634

40. Schrödinger, L. (2015). *The PyMOL Molecular Graphics System Version 2.3*.

41. Bálint, M., Jeszenői, N., Horváth, I., van der Spoel, D., & Hetényi, C. (2017). Systematic exploration of multiple drug binding sites. *Journal of Cheminformatics*, *9*(1), 65. https://doi.org/10.1186/s13321-017-0255-6

42. van Zundert, G. C. P., Rodrigues, J. P. G. L. M., Trellet, M., Schmitz, C., Kastritis, P. L., Karaca, E., Melquiond, A. S. J., van Dijk, M., de Vries, S. J., & Bonvin, A. M. J. J. (2016). The HADDOCK2.2 Web Server: User-Friendly Integrative Modeling of Biomolecular Complexes. *Journal of Molecular Biology*, *428*(4), 720–725. https://doi.org/10.1016/j.jmb.2015.09.014

43. Honorato, R. V., Koukos, P. I., Jiménez-García, B., Tsaregorodtsev, A., Verlato, M., Giachetti, A., Rosato, A., & Bonvin, A. M. J. J. (2021). Structural Biology in the Clouds: The WeNMR-EOSC Ecosystem. *Frontiers in Molecular Biosciences*, *8*. https://doi.org/10.3389/fmolb.2021.729513

44. Xue, L. C., Rodrigues, J. P., Kastritis, P. L., Bonvin, A. M., & Vangone, A. (2016). PRODIGY: a web server for predicting the binding affinity of protein–protein complexes. *Bioinformatics*, *32*(23), 3676–3678. https://doi.org/10.1093/bioinformatics/btw514

45. Yepes-Molina, L., Bárzana, G., & Carvajal, M. (2020). Controversial regulation of gene expression and protein transduction of aquaporins under drought and salinity stress. *Plants*, *9*(12), 1662. https://doi.org/10.3390/plants9121662

46. Abinaya, R. V., & Viswanathan, P. (2021). Chapter 2 - Biotechnology-based therapeutics. In Y. Hasija (Ed.), *Translational Biotechnology* (pp. 27–52). Academic Press. https://doi.org/https://doi.org/10.1016/B978-0-12-821972-0.00019-8

47. Nicolas-Espinosa, J., & Carvajal, M. (2022). Genome-wide identification and biological relevance of broccoli aquaporins. *The Plant Genome*, *15*(4). https://doi.org/10.1002/tpg2.20262

48. Damasceno, L. M., Huang, C. J., & Batt, C. A. (2012). Protein secretion in Pichia pastoris and advances in protein production. *Applied Microbiology and Biotechnology*, *93*, 31–39. https://doi.org/10.1007/s00253-011-3654-z

49. Kozak, M. (1984). Point mutations close to the AUG initiator codon affect the efficiency of translation of rat preproinsulin in vivo. *Nature*, *308*, 241–246. https://doi.org/10.1038/308241a0

50. Öberg, F., Ekvall, M., Nyblom, M., Backmark, A., Neutze, R., & Hedfalk, K. (2009). Insight into factors directing high production of eukaryotic membrane proteins; Production of 13 human AQPs in Pichia pastoris. *Molecular Membrane Biology*, *26*(4), 215–227. https://doi.org/10.1080/09687680902862085

51. Bill, R. M., & Hedfalk, K. (2021). Aquaporins – Expression, purification and characterization. *Biochimica et Biophysica Acta - Biomembranes*, *1863*(9), 183650. https://doi.org/10.1016/j.bbamem.2021.183650

52. Törnroth-Horsefield, S., Wang, Y., Hedfalk, K., Johanson, U., Karlsson, M., Tajkhorshid, E., Neutze, R., & Kjellbom, P. (2006). Structural mechanism of plant aquaporin gating. *Nature*, *439*, 688–694. https://doi.org/10.1038/nature04316

53. Oberg, F., & Hedfalk, K. (2013). Recombinant production of the human aquaporins in the yeast Pichia pastoris (Invited Review). *Molecular Membrane Biology*, *30*(1), 15–31. https://doi.org/10.3109/09687688.2012.665503

54. Al-Jubair, T., Steffen, J. H., Missel, J. W., Kitchen, P., Salman, M. M., Bill, R. M., Gourdon, P., & Törnroth-Horsefield, S. (2022). High-yield overproduction and purification of human aquaporins from Pichia pastoris. *STAR Protocols*, *3*(2), 101298. https://doi.org/https://doi.org/10.1016/j.xpro.2022.101298

55. Sabir, F., Leandro, M. J., Martins, A. P., Loureiro-Dias, M. C., Moura, T. F., Soveral, G., & Prista, C. (2014). Exploring three PIPs and three TIPs of grapevine for transport of water and atypical substrates through heterologous expression in aqy-null yeast. *PLoS ONE*, *9*(8), e102087. https://doi.org/10.1371/journal.pone.0102087

56. Yaneff, A., Vitali, V., & Amodeo, G. (2015). PIP1 aquaporins: Intrinsic water channels or PIP2 aquaporin modulators? *FEBS Letters*, *589*(23), 3508–3515. https://doi.org/10.1016/j.febslet.2015.10.018

57. Qiu, F., Mhanna, R., Zhang, L., Ding, Y., Fujita, S., & Nelson, B. J. (2014). Artificial bacterial flagella functionalized with temperature-sensitive liposomes for controlled release. *Sensors and Actuators, B: Chemical*, *196*, 676–681. https://doi.org/10.1016/j.snb.2014.01.099

58. Qi, S., Wang, R., Chaitra, G. K. M., Torres, J., Hu, X., & Fane, A. G. (2016). Aquaporin-based biomimetic reverse osmosis membranes: Stability and long term performance. *Journal of Membrane Science*, *508*, 94–103. https://doi.org/10.1016/j.memsci.2016.02.013

59. Rosa, M., Roberts, C. J., & Rodrigues, M. A. (2017). Connecting High-Temperature and lowtemperature protein stability and aggregation. *PLoS ONE*, *12*(5), e0176748. https://doi.org/10.1371/journal.pone.0176748

60. Ratz-Łyko, A., & Arct, J. (2019). Resveratrol as an active ingredient for cosmetic and dermatological applications: a review. *Journal of Cosmetic and Laser Therapy*, *21*(2), 84–90. https://doi.org/10.1080/14764172.2018.1469767

61. Ong, S. G. M., Ming, L. C., Lee, K. S., & Yuen, K. H. (2016). Influence of the encapsulation efficiency and size of liposome on the oral bioavailability of griseofulvin-loaded liposomes. *Pharmaceutics*, *8*(3). https://doi.org/10.3390/pharmaceutics8030025

62. Ghorbani Gorji, E., Rocchi, E., Schleining, G., Bender-Bojalil, D., Furtmüller, P. G., Piazza, L., Iturri, J. J., & Toca-Herrera, J. L. (2015). Characterization of resveratrol-milk protein interaction. *Journal of Food Engineering*, *167*, 217–225. https://doi.org/10.1016/j.jfoodeng.2015.05.032

63. French, K. C., Antonyak, M. A., & Cerione, R. A. (2017). Extracellular vesicle docking at the cellular port: Extracellular vesicle binding and uptake. *Seminars in Cell & Developmental Biology*, *67*, 48–55. https://doi.org/10.1016/j.semcdb.2017.01.002

ACKNOWLEDGEMENTS

The authors thank Lund University (Sweden), specifically the Division of Biochemistry and Structural Biology (Department of Chemistry), for hosting L. Yepes-Molina for a three-month period.

FUNDING

This study formed part of the AGROALNEXT programme and was supported by Spanish Ministerio de Ciencia e Innovación with funding from European Union NextGenerationEU (PRTR-C17.I1) and by Fundación Seneca with funding from Comunidad Autónoma Región de Murcia (CARM). L. Yepes-Molina was funded by PhD student grant, (FPU17/02261) and complementary mobility grant for beneficiaries of the FPU programme, (EST18/00178). UJ gratefully acknowledges funding from Formas, Olle Enkvists stiftelse and the Crafoord foundation.

TABLES

Table 1. Characteristic of liposomes and BoPIP1;2 and BoPIP2;2 proteoliposomes. Size (nm), polydispersity index (PDI), rate constant (s^{-1}), and osmotic water permeability (Pf, µm s^{-1}). Data are mean ± SE (n = 3). Different letters indicate significant differences between conditions for each sample according to one-way ANOVA followed by Tukey-HDS test ($p<0.05$).

	Size (nm)	PDI (0-1)	Rate constant (s^{-1})	Pf (µm s^{-1})
Liposomes	296.95 ± 36.20 a	0.34 ± 0.04 a	4.21 ± 0.62 a	115.75 ± 17.10 a
BoPIP1;2 proteoliposomes	255.63 ± 20.62 a	0.32 ± 0.01 a	3.76 ± 0.25 a	89.11 ± 5.93 a
BoPIP2;2 proteoliposomes	278.80 ± 37.50 a	0.33 ± 0.02 a	9.66 ± 0.79 b	249.38 ± 20.46 b

679 **Table 2. Physicochemical characterization of resveratrol extract in liposomes and BoPIP2;2**
680 **proteoliposomes.** Entrapment efficiency (EE, %), size (nm), polydispersity index (PDI), and antioxidant
681 activity (DPPH, µM TE g^{-1}). Data are mean ± SE (n = 3-5). Different letters indicate significant differences
682 between samples according to one-way ANOVA followed by Tukey-HDS test ($p<0.05$).

	EE (%)	Size (nm)	PDI	DPPH (µM TE g^{-1})
Free resveratrol extract	/	/	/	1578.34 ± 167.27 a
Liposomes	/	218.93 ± 7.99 a	0.46 ± 0.02 ab	/
BoPIP2;2 proteoliposomes	/	267.83 ± 8.05 ab	0.53 ± 0.03 a	/
Liposomes with resveratrol extract	23.17 ± 3.51 a	223.10 ± 7.56 a	0.22 ± 0.05 c	1624.84 ± 121.88 a
BoPIP2;2 proteoliposomes with resveratrol extract	52.31 ± 3.35 b	315.90 ± 7.15 b	0.36 ± 0.01 b	1426.92 ± 118.92 a

683
684

685 **Table 3. Resveratrol interactions with aquaporin**. The data correspond to the different docking poses of
686 resveratrol in Figure 3. The free energy of binding (ΔG) and the dissociation equilibrium constant (Kd) of
687 resveratrol are shown.

Pose #	ΔG (kcal/mol)	Kd (nM)	Amino acid residues within 2.5 Å of the ligand				
1	-5.58	80	GLU65A	CYS69A	SER71A	SER71C	
2	-5.34	120	LYS64A	LYS138A	ALA139A	LYS142A	ASN160D
3	-5.19	160	LYS64B	LYS142B	ASN160C	THR163C	
4	-4.97	230	SER154B	LYS64D	GLY70D		
5	-4.97	230	GLY61A	LYS64A	THR66A	SER154D	
6	-4.94	240	ASN160A	THR163A	ALA139C	LYS142C	
7	-4.91	250	LYS64B	GLU65B	ALA152C	SER154C	
8	-4.89	260	ASN160B	THR163B	LYS64D	ALA139D	
9	-4.87	270	VAL68A	VAL67D	CYS69D	GLY70D	
10	-4.81	300	VAL67B	CYS69B	SER71B	GLU65D	
11	-4.80	300	ALA152A	GLY218A	ARG225A	GLU65C	
12	-4.75	330	GLU65B	GLU65C	VAL67C	GLY70C	
13	-4.49	510	HIS62B	SER63B	PHE148B	GLY218B	ARG225B

688
689
690
691
692

693 **Table 4. Integrin-aquaporin interactions**. The data correspond to the docking pose shown in Figure 4.
694 Amino acid residues are selected within 3.5 Å.

Integrin	Aquaporin	Distance (Å)
ARG220A	VAL155A	3.37
ARG220A	LYS237A	1.71
SER224A	GLN147A	2.18
TYR226A	VAL67C	3.42
ASN256A	VAL68C	3.29
ARG271A	VAL155A	3.37
ARG271A	GLY158A	3.21
ARG271A	TYR159A	2.71
ARG271A	LYS237A	3.00
SER272A	GLY158A	2.49
TYR274A	GLY143C	3.46
TYR274A	GLN147C	2.86
ASN275A	THR66C	2.43
ASN275A	GLN147C	3.24
ALA332A	ASN146C	2.35
ILE334A	GLN147C	2.71
GLU335A	ASN146C	3.03
GLU335A	GLN147C	2.75
PRO336A	GLN147C	2.71
PRO336A	PHE148C	3.48
GLU319B	VAL67A	3.08
GLU320B	THR66A	3.33
LYS326B	VAL68D	2.56

695
696
697
698
699
700
701
702
703
704
705
706
707
708
709
710

FIGURE LEGENDS

Figure 1. Optimization of BoPIP1;2 and BoPIP2;2 purification from Pichia *pastoris*. (**A**) Western-blot with crude cell extract of five clones from each zeocin level (100, 500, and 1000 µg zeocin mL^{-1}) for BoPIP1;2 and BoPIP2;2. (**B**) Western-blot with the three clones exhibiting the highest expression. Asterisks indicate the selected clones for further trials. (**C**) pPICZB vector scheme with a BoPIP encoding insert. (**D**) OD_{600} of samples from the fermenter at different time points. (**E-F**) Western-blot for BoPIP1;2 and BoPIP2;2 of crude cell lysates at different time points. (**G**) Coomassie-stained SDS-PAGE gel and (**H**) western-blots showing the positive control (C+), flow-through (FT), wash fractions (W), and elution fractions (E0, E1, and E2) obtained from the Ni-NTA His trap column during the protein purification process.

Figure 2. Stability and functionality of liposomes and proteoliposomes over time. (**A**) Relative change in size and (**B**) polydispersity index (PdI) of empty liposomes, BoPIP1;2 proteoliposomes, and BoPIP2;2 proteoliposomes compare to time 0 during storage for two and seven days at 4 °C, 20 °C, and 37 °C. Asterisks indicate significant differences in each sample at each time and temperature compared to the initial time. (**C**) Osmotic water permeability (Pf) and (**D**) western-blots of liposomes, BoPIP1;2 proteoliposomes, and BoPIP2;2 proteoliposomes analysed after storage for seven days at different temperatures. Different letters indicate significant differences among conditions for each sample according to one-way ANOVA followed by Tukey-HDS test ($p<0.05$). Asterisks (*) indicate significant differences between both BoPIP1;2 and BoPIP2;2 proteoliposomes, and empty liposomes for each condition according to Student t-test ($p<0.05$). Data are mean ± SE (n = 3).

Figure 3. Resveratrol encapsulation in liposomes and proteoliposomes and resveratrol-aquaporin docking. (**A**) Entrapment efficiency (%) of resveratrol extract in liposomes and BoPIP2;2 proteoliposomes, and (**B**) antioxidant activity of free resveratrol extract and encapsulated extract after storage for 15 and 30 days. Data are mean ± SE (n = 3). Different letters in (A) indicate significant differences according to one-way ANOVA followed by Tukey-HDS test ($p<0.05$). Different letters in (B) indicate significant differences among different days for each sample according to one-way ANOVA followed by Tukey-HDS test ($p<0.05$), and asterisks (*) indicate significant differences between both empty liposomes and BoPIP2;2 proteoliposomes, and free resveratrol extract according to Student t-test (*$p<0.05$, ** $p<0.01$). (**C**) Docking of resveratrol to the outer face of aquaporin tetramer showing multiple binding conformations. Resveratrol carbon backbone is shown in green, the conformation of lowest free energy of binding is represented in spheres and the rest in sticks. Aquaporin chains are depicted in green, cyan, magenta, and yellow for A, B, C, and D chains, respectively. In light blue sticks, Cys69 residues are represented forming disulphide bridges. (**D**) Close-up of the interaction region of the docking conformation of the lowest energy of binding (pose 1 in Figure 3C). Resveratrol carbon backbone is in orange, and the amino acid residues are colored as their corresponding chains. Interaction distances (Å) are in dashed lines.

Figure 4. Integrin-aquaporin docking. (**A**) Docking of Integrin-Aquaporin complex showing the best scoring docking pose obtained from HADDOCK server (score=-373.70). The predicted free energy of binding calculated with was -10.4 kcal/mol corresponding to a Kd=24 nM). Aquaporin is shown in orange (chains A, B, C and D), and integrin in green (chain A or Integrin alpha-5) and blue (chain B or Integrin beta-1) . Metal ions are shown as spheres, Mg^{2+} in magenta, and Ca^{2+} in yellow. (**B**) Close-up of the interaction region of the docking conformation. The amino acid residues are colored as their corresponding chains (Figure 4A).